Synthesis, Characterization and Catalytic Activity of Single Site, Lewis Acidic Aluminosilicates

Ales Styskalik*,[a,b] Joshua G. Abbott,[c] Damien P. Debecker[d], Craig E. Barnes*[a]

[a]University of Tennessee, Department of Chemistry, Knoxville, TN 37996-1600, United States.

[b]Masaryk University, Department of Chemistry, Kotlarska 2, CZ-61137 Brno, Masaryk University, CEITEC MU, Kamenice 5, CZ-62500 Brno, CZ;

[c]Xtalic Corporation, 260 Cedar Hill Street, Marlborough, MA 01752 (JAbbott@xtalic.com);

[d]Institute of Condensed Matter and Nanoscience - Molecules, Solids and reactivity (IMCN/MOST), Université catholique de Louvain, Croix du Sud 2/17, 1348 Louvain-La-Neuve, Belgium (damien.debecker@uclouvain.be)

*Corresponding authors. E-mail address: cebarnes@utk.edu (C. E. Barnes), Phone: +18659743446; 211138@mail.muni.cz (A. Styskalik)

Keywords: heterogeneous catalysis; single site, aluminosilicate, Lewis acid, solid acid

ABSTRACT

A general synthetic strategy for the preparation of atomically dispersed, well-defined Lewis acidic aluminum sites in silicate matrices is described and illustrated. These amorphous matrices are composed of the spherosilicate cubes (Si_8O_{20}) linked together by combinations of aluminum and siloxane groups. The connectivity of the catalytically active aluminum centers to the surrounding silicate matrix can be varied by choice of aluminum precursor. "Extraframework" 3-connected Al←Py and Al←THF sites are obtained from the corresponding $AlCl_3$·L complexes and 4-connected "framework" sites from Y[$AlCl_4$] (Y = Lutidinium, $[Bu_4N]^+$). The aluminum sites in these porous silicates are characterized by gravimetry, IR and multinuclear SSNMR spectroscopies as well as ligand exchange reactions. Their catalytic activities as Lewis acids are investigated for the aminolysis of styrene oxide by aniline. These single site aluminosilicate catalysts exhibit activities that are comparable to or better than analogous, well-known zeolite and amorphous aluminosilicate materials. Their activities are dependent on the connectivity of

aluminum to the surrounding silicate matrix as well as the length and flexibility of secondary linkers in the matrix.

Introduction

While homogeneous catalysts are generally better understood than heterogeneous analogues, the latter are frequently preferred in large scale chemical industries due to ease of separation and recovery of the catalyst and ready adaptation to continuous flow processes.[1, 2] Despite these advantages, a long-standing challenge in heterogeneous catalysis has been the precise identification of the active sites responsible for catalysis. This challenge is exacerbated by the fact that traditional methods of creating surface active sites often lead to the formation of a number of different but similar sites, some of which show reduced activity or selectivity for the desired reaction. In this context, the advantages of well defined, single site catalysts are obvious.[3] Characterization is simplified when the spectral signatures of multiple sites do not require deconvolution. As a result, counting sites and developing a fundamental understanding of the mechanisms of catalysis are much easier. Single site catalysts are also expected to be more specific for the substrates they accept and more selective for the products they produce. Finally, a well-defined, single site catalyst is an ideal starting point for computational modeling which has now become an integral part of catalysis science.[4-6]

The combination of these factors has led to increased interest in the targeted synthesis of single site catalysts.[7, 8] The preparation of dense arrays of identical active sites on the surfaces of porous solids remains challenging, however, as the inherent heterogeneity of surface functionalities or their uneven distribution across oxide support surfaces makes it difficult to distinguish between rigorous single site catalysts or materials exhibiting distributions of similar sites. Strategies to overcome these obstacles include thermal conditioning of oxide supports[9, 10] and chemical modification of support surfaces to tailor the number and distribution of surface hydroxy groups.[11] Direct grafting and tethering of catalytically active complexes onto traditional support surfaces have led to a number of recent advancements in this area.[7, 8]

Aluminosilicates, both zeolitic and amorphous, represent an important family of solid acid catalysts for both academic study and industrial application.[12-14] This broad applicability has led to extensive efforts to synthesize and characterize well defined aluminum sites within silicate networks.[15-23]

"Framework" aluminum sites are isolated aluminum atoms embedded (4-connected to the surrounding matrix) in the silicate scaffolding. They are generally believed to be the main Brønsted site in aluminosilicates when the counterion is a proton (**I**).[24] In most aluminosilicates other types of aluminum sites also are present which are frequently described as "extraframework aluminum species".[14, 25-27] These range from isolated aluminum atoms that are not totally embedded in the silicate framework to small domains of alumina that exist outside of the silica matrix, whether zeolitic or amorphous. Much less is known about the roles this broad collection of potential active sites play in the catalysis exhibited by aluminosilicates but they are known to be important in the reactions they catalyze.[14] The frequent combination of both framework and extraframework active sites in aluminosilicates is a good illustration of the challenges one faces when attempting to answer the question of what the active site is in a heterogeneous catalyst.

An approach to addressing these challenges begins with the premise that the active sites in solid phase catalysts should be clearly identified and a rational synthetic scheme developed to produce only the targeted site throughout the matrix, similar to targeting a molecular catalyst in homogeneous systems. In extending this strategy to heterogeneous systems several new requirements must be met. In a solid phase catalyst, the active sites reside on the surfaces of the solid and must be easily accessed by reagents in fluid phases (gas or liquid). Furthermore, high densities of targeted surface sites must also be achieved while keeping them isolated from one another to prevent interactions that might create new sites which exhibit undesired catalytic activities. It is with these objectives in mind that we have developed a general synthetic methodology for the preparation of porous solid matrices containing arrays of identical active sites for catalysis.[28, 29]

Herein we describe the targeted synthesis of porous aluminosilicate catalysts that contain different types of aluminum sites. The first contain only 3-connected "extraframework", Lewis acidic sites and the second, only 4-connected framework sites (**I** and **II**). The sites in these porous materials are characterized by a variety of spectroscopic and analytical techniques as well as ligand exchange reactions. Their activities as catalysts in the aminolysis of styrene oxide with aniline are described.

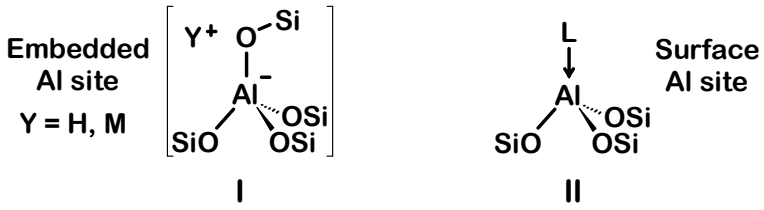

Experimental

General experimental details, instrumentation and a complete summary of spectroscopic data are found in the supporting material to the manuscript. These may be accessed at the journal website.

Catalyst Synthesis:

Synthesis of 3-connected aluminum sites in Si_8O_{20}-based building block matrices with disiloxy ethane bridges ((**1**) Figure 1): 1.999 g (1.077 mmol) dehydrated $(Me_3SnO)_8Si_8O_{12}$ (trimethyltin cube) was loaded in a Schlenk vessel in a glove box and sealed. 20 cm^3 THF was then delivered to the reaction vessel and stirred until a homogeneous solution was obtained. In a separate Schlenk vessel, a THF solution of 0.141 g (1.06 mmol) $AlCl_3$ was prepared and kept at −78 °C. 0.086 g (1.087 mmol) pyridine was then added to the $AlCl_3$ solution which was warmed and stirred at RT for 15 min. The solution of Py·$AlCl_3$ was then added via syringe to the solution of the trimethyltin cube with vigorous stirring. The reaction was heated at 60 °C for 48 h forming a hazy solution of aluminosilicate oligomers.

Al-connectivity to silicate cubes was determined by collecting all volatiles under vacuum in an external cold trap. The only byproduct observed in the volatiles was trimethyltin chloride (NMR, GCMS). The mass change in the reaction then defined the number of chlorides lost by aluminum in this first cross-linking step.

The oligomers formed at this stage were redissolved in solvent and further cross-linked together with a silyl chloride reagent such as 1,2 *bis*(dimethylchlorosilyl) ethane (0.473 g; 2.217 mmol) (conditions: 60 °C; 48 h) producing a milky gel. After heating, the solvent and byproduct, Me_3SnCl, were again removed under vacuum (60 °C) for 24 h giving 1.176 g of a white xerogel product (**1**).

Gravimetric determination of the total number of chloride groups reacted for both cross-linking steps (exp. Me_3SnCl/theo. Me_3SnCl) gave 100.4 %. Gravimetric analysis for this material gave an aluminum wt% of 2.43% while elemental analysis (ICP-OES) gave an aluminum content of 2.23 wt%.

At this point in the synthesis it is estimated that one Me_3Sn group remains unreacted per cube in the matrix, making the Al:Sn ratio ~1.0. Although residual trimethyltin groups were found to have no effect on the catalytic activities of these materials, they could be removed via reaction with HCl-free

chlorotrimethylsilane (TMSCl). Reaction of a 3:1 molar ratio (TMSCl : residual tin group) at 60 °C for 12 h gave rise to Sn-free xerogels (Al : Sn ratio ~60, ICP-OES, Table 1).

3-connected aluminosilicate xerogels **2, 5** and **6** were synthesized in a similar manner to the pyridine adduct of aluminum trichloride. In the reaction of THF·$AlCl_3$ with the tin cube, it is necessary to keep the reaction solution at −78 °C while adding $AlCl_3$ in order to avoid side reactions (e.g. THF ring opening). The initial reaction mixture was kept at −78 °C for 12 h whereupon the temperature was slowly raised to 60 °C to complete the condensation.

The effect of varying the size and rigidity of the secondary linker on catalysis activity was investigated. The ethylene bridge disiloxane (Figure 1) was used to prepare xerogels **1** – **4**, while dimethyl siloxane linker was used in the case of xerogel **5** and 1,3-(dimethylsiloxy) propane in the case of xerogel **6**. The conditions used to perform all secondary cross-linking steps were identical to those described above.

Aluminosilicate **1a** was prepared from xerogel **2** by the exchange of THF for pyridine at the Al sites in the xerogel. 0.279 g of xerogel **2** (0.222 mmol Al) was reacted with pyridine (0.035 g, 0.445 mmol; 2 eq pyridine per Al site) in 5 cm^3 toluene at 60 °C overnight. The solvent and excess pyridine were then removed *in vacuo* and the xerogel was dried overnight at 60 °C providing a white solid **1a**.

Synthesis of 4-connected "embedded" aluminum sites in Si_8O_{20}-based building block matrices: Xergels **3** and **4** containing different counterions to the $[Al(OSi)_4]^-$ site were synthesized in a manner similar to xerogel **1** from $[Bu_4N][AlCl_4]$, and $[LuH][AlCl_4]$, respectively. Gravimetric analyses after the first cross-linking are consistent with 4-connected Al centers in these xerogels (Table 1).

Precursor loadings, yields, and metal contents for the resulting xerogels are summarized in Table 1.

Table 1 Synthesis and ICP-OES Analysis Data for Aluminosilicate Catalysts

Xerogel	Al site	n_{Al} (mmol)	n_{Cube} (mmol)	n_{linker} (mmol)	Al wt%[a] theo/exp	Si/Al[b] ratio	Al/Sn[a] ratio	Al-connectivity theo/exp[e]
1	3C-Al←Py	1.06	1.077	2.22	2.43/2.23	12	57	3/2.78
2	3C-Al←THF	0.502	0.537	1.11	2.25/2.07	13	92	3/2.73
3[c]	4C-Al·Bu_4N^+	0.267	0.406	0.815	1.40/1.43	18	0.32	4/-
4[c]	4C-Al·LuH^+	0.343	0.449	0.881	2.11/1.74	16	0.50	4/4.17

5[c,d]	3C-Al←THF	0.652	0.799	1.51	1.99/2.29	14	0.50	3/2.73
6[c,f]	3C-Al←THF	0.600	0.791	1.58	1.82/1.77	16	0.44	3/2.73

[a]Experimental values from ICP-OES analyses; [b]based on reagent stoichiometry; [c]Me_3Sn groups not removed; [d]Me_2SiCl_2 used as second cross-linker; [e]gravimetric data based on $ClSnMe_3$ formed in first cross-linking step; [f]1,3 bis(dimethylchlorosilyl) propane used as second cross-linker.

Reactions of triethylphosphate (TEPO) with xerogels **4** and **6**: Samples were exposed to the TEPO in toluene at 60°C for 24 hours after which all volatiles were removed (50°C). Solid state NMRs were prepared and data were collected under air free conditions.

Catalysis Protocol. The products of the aminolysis of styrene oxide with aniline are shown in equation 1.

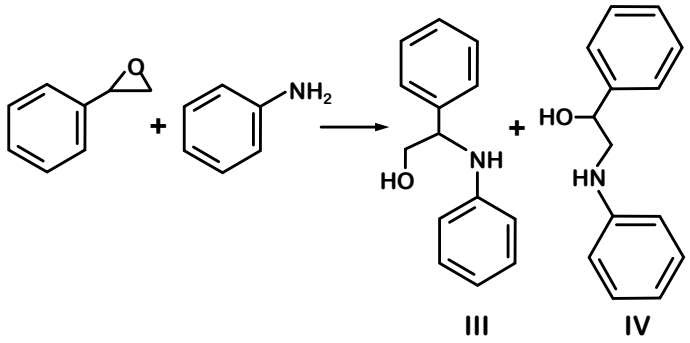

Equation 1

Catalysis reaction mixtures consisted of catalyst (aluminosilicate xerogel, *ca.* 25 mg, 0.02 mmol Al), dry toluene (5 cm^3), styrene oxide (0.587 cm^3, 5.00 mmol), and aniline (0.456 cm^3, 5.00 mmol). The substrate to aluminum ratio was ~250 in all cases. All reactions were heated at 50 °C and stirred continuously at 400 rpm. Reaction products were quantified via proton NMR spectroscopy after 15 min using tetramethylsilane as an internal standard. To investigate Al leaching, ~150 mg of either catalyst **1** or **5** was used in regular catalytic reaction mixture for 2 h. After centrifugation and filtering away the catalyst powder, the filtrate was dried *in vacuo*, oxidized and digested with HNO_3 and tested for the presence of Al by ICP-OES. The recyclability of the catalyst was studied by washing the used catalyst with toluene and drying under vacuum at 60 °C. The material was then reused as a catalyst in the aminolysis reaction. This procedure was repeated three times with xerogels **1** and **5**.

Results and discussion

Single-Site Strategy and Characterization: The strategy described here for constructing aluminosilicate catalysts with atomically dispersed aluminum atoms is similar to our previous work involving single-site

metallosilicates[30, 31] and rests upon three basic tenets: (1) the availability of linking reagents and a silicate building block; (2) the ability to cleanly link the two together; and (3) a simple sequential addition strategy by which the specific connectivity of the aluminum centers between building blocks can be targeted in the final matrix.

Figure 1illustrates the steps of the strategy for xerogel **1**. In the first cross-linking step, trialkyl tin groups on the terminal oxygens of the Si_8O_{20} core cleanly react with the chloride ligands of Py·$AlCl_3$ to produce Si–O–Al linkages (Dose 1, Figure 1).[31, 32] Based on gravimetric analysis of the trimethyltin chloride by-product, all chlorides on aluminum are found to be reactive leading exclusively to a 3-connected aluminum center linking three cube together.

The highest ratio of chloride to Me_3Sn groups in this first cross-linking step that can be used and still achieve reaction of all chloride ligands on aluminum is 3:8 (i.e. 1 Py·$AlCl_3$: 1 cube). The connectivity drops off at higher ratios presumably due to the increasing oligomer size and rigidity as more cross-links are formed. It is important to note that reaching the limiting connectivity for aluminum in this first cross-linking step is critical to achieving identical catalytic sites throughout these matrices.

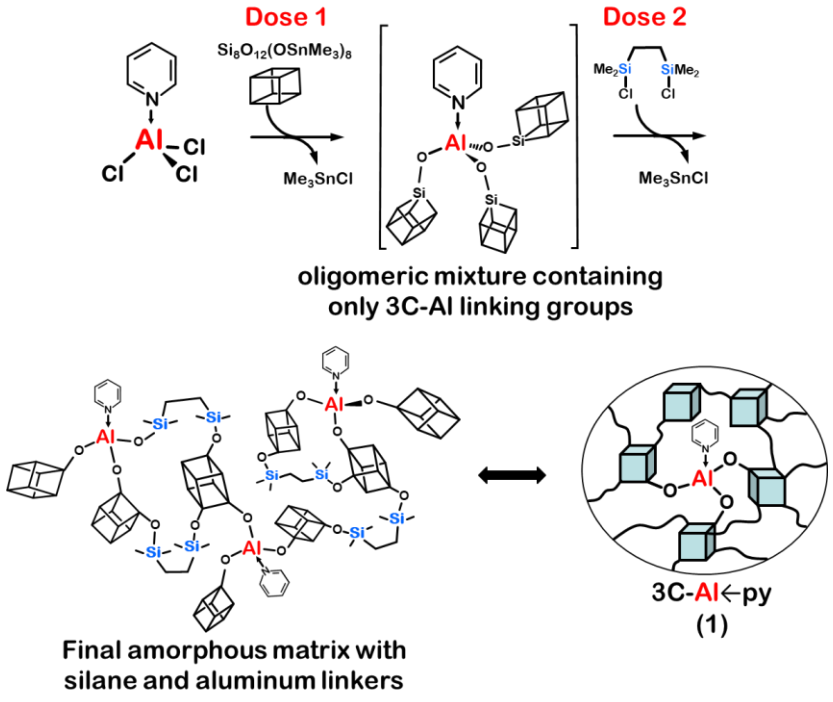

Figure 1 Synthetic scheme for preparing aluminum sites targeting connectivity to the surrounding matrix of Si_8O_{20} cubes.

The second step involves further cross-linking with a reagent that will produce chemically and thermally robust bonds to hold the matrix together while not affecting the active sites. Chlorosilanes are ideal for this purpose (Dose 2, Figure 1).[30] Three different linking groups were used in the preparation of these catalysts to probe the influence of size and rigidity on the surface area, porosity and catalytic activity. Dichlorodimethylsilane was the shortest and most rigid secondary cross-linker investigated (xerogel **5**). The ethylene bridged linker –$OSiMe_2$-CH_2CH_2-$SiMe_2O$– was used in the preparation of xerogels **1** – **4**. The longest and most flexible linker had a 1,3 disiloxane propyl group bridging different cubes in the matrix (**6**).

The last step in the synthesis of these nanostructured catalysts involves removing the remaining tri-methyltin groups from the matrix by reaction with TMSCl to produce a robust, hydrophobic surface of TMS groups grafted onto the aluminosilicate catalysts. During synthesis, all of the steps described above were followed by gravimetric and ICP-OES analyses.

In the manner just described, a series of matrices containing atomically dispersed 3C- and 4C-aluminum sites within a framework of cross-linked silicate building blocks were prepared (Table 1, Figure 2). Under the synthesis conditions (reaction temperatures <60 °C) and assuming cube corners react independently of each other, the formation of cross-links will be both random and irreversible, thus leading to amorphous glasses. The lack of long range order was verified by PXRD scans on several samples.

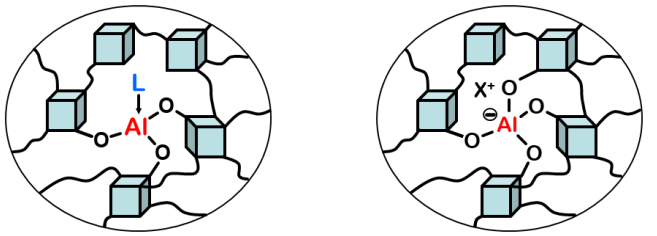

Figure 2 3-connected (3C) and 4-connected (4C) aluminum(III) sites in the xerogels **1** – **4**

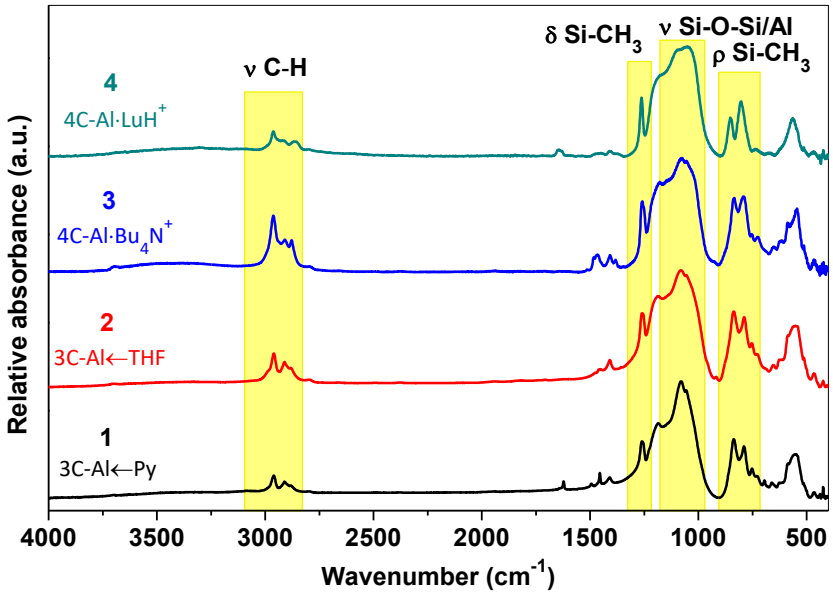

Figure 3 IR spectra of dried aluminosilicate catalysts

Infrared spectra of the dried xerogels are shown in Figure 3. Of note is the lack of vibrational bands for OH groups, around 3400 cm^{-1} and 950 cm^{-1}. This is consistent with the rigorous non-aqueous synthesis conditions.[33] Strong CH_3 symmetric bending and rocking vibrations at 1261 and 839/754 cm^{-1} are assigned to Si–CH_3 groups.[34] Similarly, IR spectra of xerogels **3** and **4** show absorption bands characteristic for tetrabutylammonium[35] (1466 and 1485 cm^{-1}) and lutidinium[36] (1628 and 1651 cm^{-1}) cations.

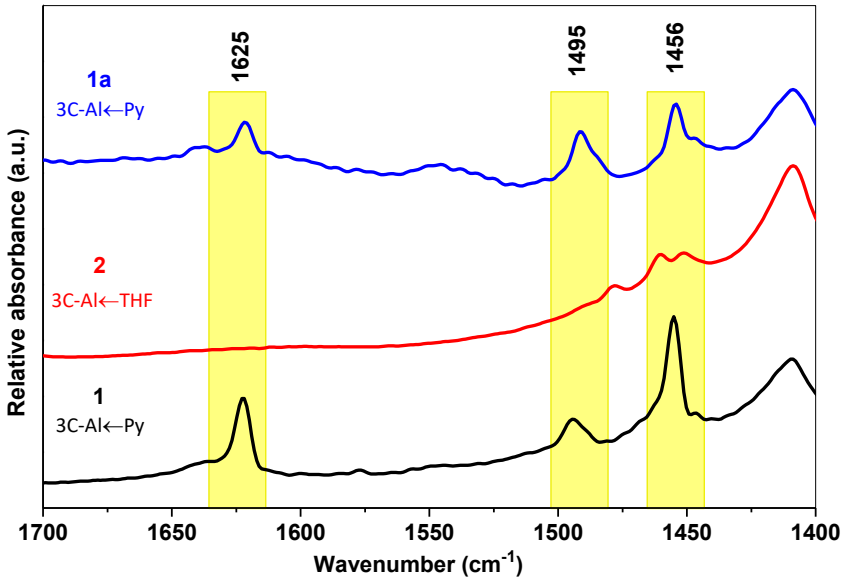

Figure 4 IR spectra of the pyridine ring vibration region of xerogels 1, 2, 1a

A prominent feature in all IR spectra is the strong band at 1082 cm^{-1} which we assign to Si–O–Si/Al bridges forming the aluminosilicate structure.[37-39] Finally, in the case of **1** prepared from Py·$AlCl_3$, distinct bands at 1456, 1495, and 1625 cm^{-1} are observed which may be assigned to Lewis acid bound pyridine[40, 41] and serve as clear evidence for the retention of pyridine coordinated to aluminum throughout the synthesis (Figure 4). No bands for Brønsted (pyridinium $[HPy]^+$) or silanols bound pyridine are observed for any of the catalysts described above.[37] Xerogel **1a**, prepared from the THF-containing xerogel **2** by the exchange with pyridine, gives rise to an IR spectrum that is virtually identical to **1** containing purely Lewis bound pyridine (Figure 4).

^{27}Al MAS NMR spectra (Figure 5) of all xerogels reveal only a single resonance at ~49 ppm. Its assignment to 4-coordinate Al species in a silicate network is well documented in the literature.[42-44] Of note is the fact that THF exchange by pyridine (2-fold excess) does not give rise to Al-SSNMR signals for higher coordination Al centers in xerogel **1a**.[45]

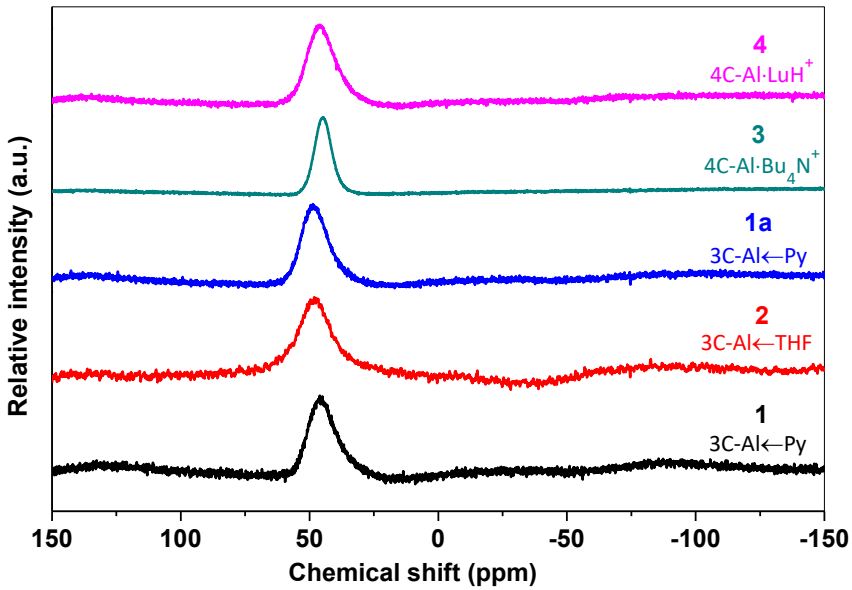

Figure 5 **^{27}Al MAS NMR spectra of aluminosilicate catalysts** 1 – 4,**.**

^{13}C NMR resonances (7, −1, and −3 ppm) for the disilyl ethane linking and trimethylsilyl (after removal of trimethyltin) groups present in xerogels **1**, **1a**, and **2** were assigned to OSiMe$_2$*CH$_2$*, OSi*Me*$_2$CH$_2$ and OSi*Me*$_3$ groups, respectively (Figure 6). Signals for pyridine aromatic ring carbons and THF ligands coordinated to 3C-Al sites were observed for xerogels **1** and **2,** respectively. Similarly, signals characteristic for tetrabutylammonium, and lutidinium were observed in the spectra of xerogels **3**, and **4**, respectively (Figure 7).

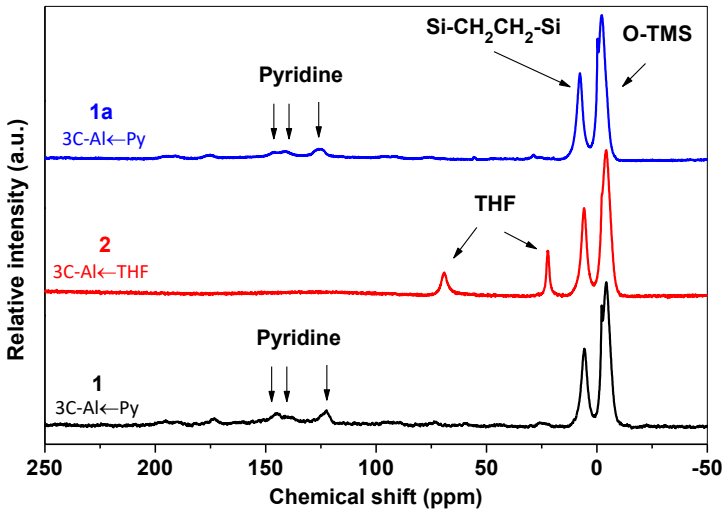

Figure 6 ^{13}C CPMAS NMR spectra of Aluminosilicate Catalysts **1, 2,** and **1a**

The ^{13}C CPMAS NMR spectrum of xerogel **1a** after exchange of THF for pyridine (2 mole eq pyridine for each Al←THF site; 12 hrs; 60 °C) showed signals of coordinated pyridine, and no signals for residual THF (eq 2). The desired reaction was further confirmed by proton NMR analyses of volatiles, which showed resonances assigned to THF and pyridine in the expected ratio after the reaction. Similar results were observed for xerogel **6** where full exchange took only 2 hr at 60 °C.

$$(\equiv SiO)_3Al \leftarrow THF \; + \; 2\,Py \;\; \rightarrow \;\; (\equiv SiO)_3Al \leftarrow Py \; + 1\,THF \; + \; 1\,Py \qquad (2)$$

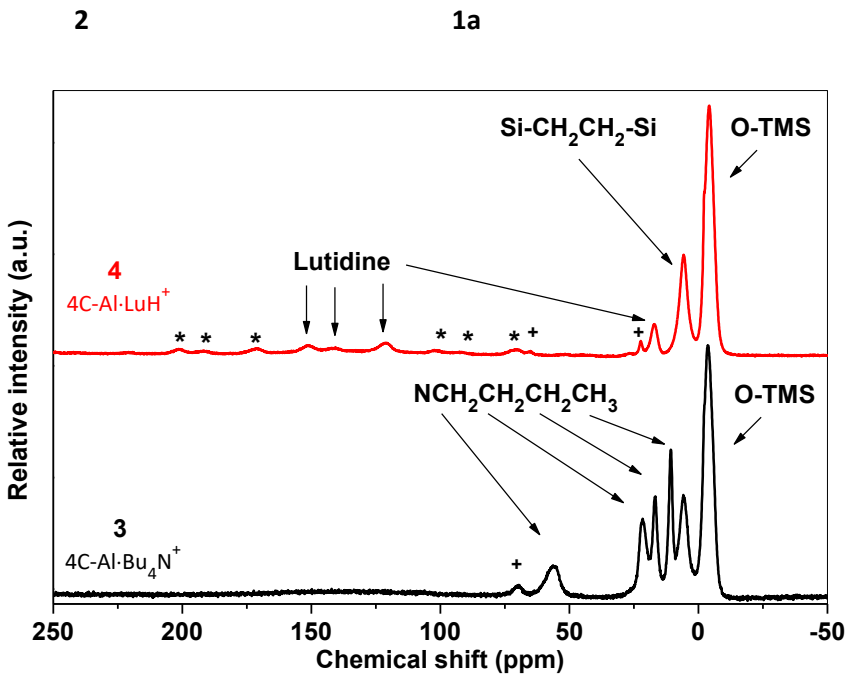

Figure 7: ^{13}C CPMAS NMR spectra for samples of aluminosilicate catalysts **3** and **4**. (* denotes spinning sidebands; + denotes residual THF after drying)

^{29}Si CPMAS NMR spectra displayed only two resonances at ~11 and ~−111 ppm (Figure 8). The signal at lower field can be assigned to O*Si*Me_3 and O*Si*Me_2CH_2 groups in these matrices. The upfield peak (−111 ppm) originates from the silicate cube and can be assigned to $(SiO)_4$*Si* moieties. A shoulder observed at −104 ppm is assigned to $(SiO)_3$*Si*OAl groups and is consistent with the presence of Si−O−Al bridges. No signals for Si−Cl or Si−OH groups (from exposure to water) were observed. Furthermore, no resonances suggesting attack and disruption of the Si_8O_{20} cage were observed.

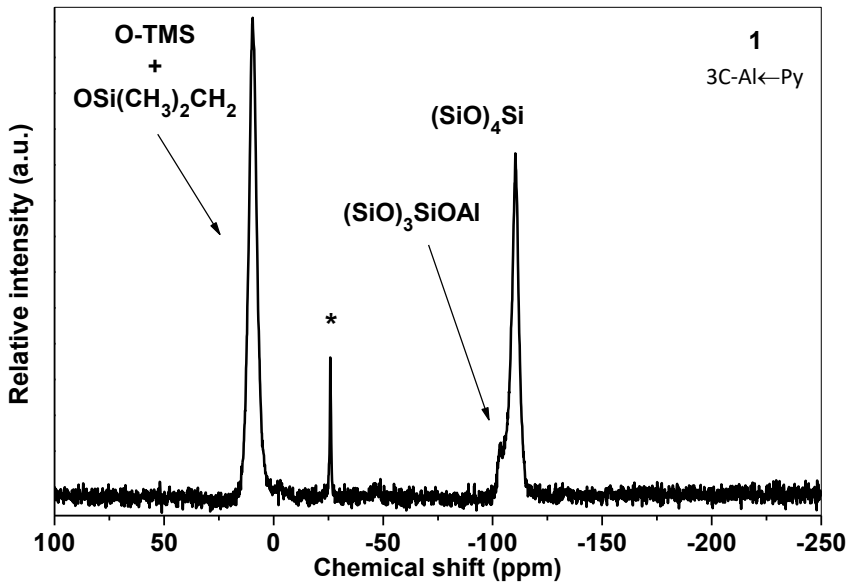

Figure 8: ^{29}Si CPMAS NMR spectrum of xerogel 1; *denotes silicon grease.

From the data presented above (IR spectroscopy, ^{1}H NMR, ^{27}Al MAS NMR, and ^{13}C, ^{29}Si CPMAS NMR), we can conclude that the sequential cross-linking synthesis strategy leads to the formation of targeted, atomically dispersed, isolated tetrahedral aluminum sites linked to either three (**1, 1a, 2, 5**, **6**) or four (**3, 4**) silicate cubes. Furthermore, THF is relatively weakly bound to the Al sites in **2** and **6** and can be cleanly exchanged for pyridine to produce the corresponding Al←py sites which are spectroscopically identical to xerogel **1**. Thus, the 3-connected THF sites in these xerogels are ideal starting points for studying the ligand exchange mechanisms that are central to their activities as catalysts.

The ligand exchange reaction observed for xerogel **5** is, however, quite different. Incomplete exchange (~50%) was observed after heating for several days. The only difference between xerogels **5** and **2/6** are the peripheral organosilane cross-linkers installed in the second cross-linking step. The smaller, single atom bridges between cubes (O–$SiMe_2$–O) in **5** appears to create a barrier to ligand exchange reactions at the aluminum sites in the matrix. This conclusion is in agreement with the lower catalytic activity of **5** compared with **2** and **6** (*vide infra*).

In order to characterize the relative strengths of 3C-Al and 4C-Al acid sites, reactions between xerogels **4** and **6**, and triethylphosphine oxide (TEPO) were investigated.[46] After exposure of each xerogel to 1.2 equivalents of TEPO (based on calculated number of Al sites in each sample) a multinuclear NMR study was conducted. ^{1}H NMR of volatiles and the ^{13}C CPMAS spectrum (Figure S1) of catalyst **6** indicate that all pyridine was lost from the aluminum sites and replaced by TEPO. This observation indicates that all aluminum sites in **6** are accessible to ligand exchange. The ^{31}P MAS spectrum (Figure 9) shows two

signals at 71.7 and 51.5 ppm in the ratio of 1: 0.17. The signal at 71.7 ppm is assigned to TEPO groups bound to the 3C-Al sites in the matrix while the signal at ~51 ppm represents physisorbed TEPO groups.[47] We interpret the signal at ~71 ppm to TEPO bound to medium strength, 3C-Al Lewis acid sites. For comparison, ^{31}P shifts for TEPO bound to various Lewis and Brønsted acids are: silica gel-$AlCl_3$ (102 ppm), Al_2Cl_6 (86.6), H-Mordenite (75.6), and silica gel (61 ppm).[47, 48] The ^{27}Al MAS spectrum (Figure S2) for this xerogel indicates that some 5- and 6-coordinate aluminum species are also formed in

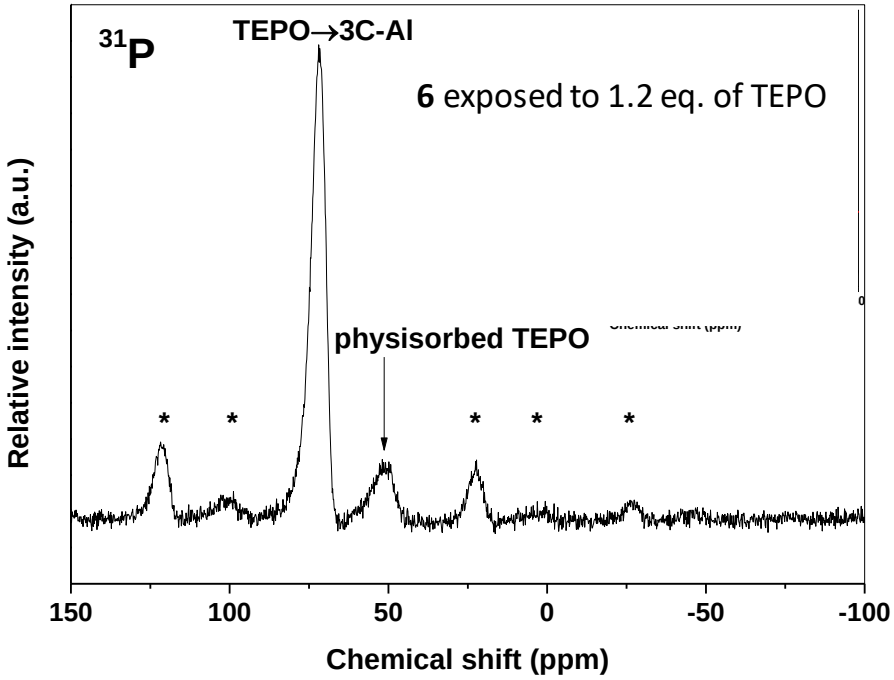

Figure 9 ^{31}P MAS spectrum of 6 exposed to 1.2 eq of TEPO. Two signals (71.8 and ~51 ppm) are observed. Features with (*) above them are spinning sidebands. Relative peak integrations are 1 : 0.17, resp.

the exchange reaction.

In contrast to these observations, xerogel **4** displays much lower ability to bind TEPO molecules as evidenced by the ^{27}Al MAS NMR where the signal for the original 4C-Al site dominates the spectrum even after reaction with 3 eq of TEPO (Figure S3). The ^{31}P MAS spectrum for xerogel **4** + TEPO (Figure S4) again shows two signals at roughly 71 and 50 ppm with a shoulder at ~58 ppm. These signals are tentatively assigned to TEPO interacting with medium strength Brønsted acid sites (lutidinium cation, 71 ppm), physisorbed TEPO (50 ppm), and TEPO bound to a weak Lewis acid (58 ppm). The 4C-Al sites in xerogel **4** are expected to be significantly more sterically congested and less flexible in creating coordination sites for substrates. Therefore, the aluminum sites bind TEPO more weakly and show less

propensity to form higher coordination geometries even in the presence of excess TEPO. Further work is underway to confirm these assignments and observations.

Nitrogen adsorption–desorption isotherms of **1**, **2**, and **5** (Figure S5) are typical for the xerogels with 3-connected Al sites described herein.[49] According to IUPAC classifications, the isotherms can be described as a mixture of type I and II isotherms indicative of the presence of both micro and mesopores. Most of the isotherms show hysteresis that does not close in the low p/p_0 range indicating that the adsorption is partially irreversible under the experimental conditions. Similar isotherms have been reported[50, 51] for xerogels based on cubic Si_8O_{12} units cross-linked with alkane and alkyl silane bridges where this behavior was attributed either to micropores with the same width at the pore entrance as that of the adsorbate molecules resulting in irreversible uptake, or to flexibility in the networks associated with swelling of a non-rigid porous structure. Both explanations are possible for the xerogels described here.

The highest apparent specific surface areas were obtained for xerogels **1a** and **2** before and after exchange of THF for pyridine (400 $m^2\ g^{-1}$; (Table 2). The corresponding total pore volume was V_{total} = 0.288 $cm^3\ g^{-1}$ (at p/p_0 = 0.98). According to t-plot analyses the pore volume of the xerogel (**1a**) consisted of 38% micropores with meso and larger pores accounting for the rest. The fraction of microporous pore volume was similar in other samples ranging from 32 to 52%. The aluminosilicate catalysts **3** and **4** with 4-connected Al sites displayed much lower surface areas.

Table 2 Surface area and pose size distribution Data for Aluminosilicate Catalysts

Xerogel	Al Site	Secondary Cross-linking agent	SA $[m^2\ g^{-1}]$	V_{total} $[cm^3\ g^{-1}]$	D[a] [nm]	MPV[b] [%]
1	3C-Al←py	$ClMe_2Si{-}CH_2CH_2{-}SiMe_2Cl$	279	0.184	2.6	32
2	3C-Al←THF	$ClMe_2Si{-}CH_2CH_2{-}SiMe_2Cl$	397	0.242	2.4	47
1a	3C-Al←Py (from **2**)	$ClMe_2Si{-}CH_2CH_2{-}SiMe_2Cl$	398	0.288	2.9	38
3	4C-Al·Bu_4N^+	$ClMe_2Si{-}CH_2CH_2{-}SiMe_2Cl$	<10	-	-	-
4	4C-Al·LuH^+	$ClMe_2Si{-}CH_2CH_2{-}SiMe_2Cl$	15	0.036	-	-
5	3C-Al←THF	Me_2SiCl_2	153	0.110	2.8	32
6	3C-Al←THF	$ClMe_2Si{-}CH_2CH_2CH_2{-}SiMe_2Cl$	255	0.139	2.2	52

[a]Average pore diameter ($4V_{total}/SA$); [b]MPV: Micropore Volume = V_{micro}/V_{total}, V_{micro} determined by t-plot analysis; V_{total} estimated at $p/p_0 = 0.98$.

Catalysis: The catalytic performance of the synthesized xerogels was tested in the aminolysis of styrene oxide with aniline (eq 1) which has been reported to be catalyzed by Lewis acids.[52-56] Proton NMR and GC-MS analyses of the reaction mixtures were used to identify two products formed (2-phenyl-2-(phenylamino)ethanol (**III**) and 1-phenyl-2-(phenylamino)ethanol) (**IV**)) which accounted for 95 – 100% of the styrene oxide consumed. All catalysts remain active while the epoxide substrate is present in the reaction mixture (Figure S6) achieving conversions in excess of 80% when run in excess of aniline.

Conversions for turnover frequency calculations were measured after 15 minutes. In blank reactions without catalyst and with Al-free silicate platforms, only negligible amounts of products were obtained after 1 h confirming that the presence of Al centers is necessary for catalytic activity. The heterogeneous nature of the catalytic reactivity displayed by these aluminosilicate catalysts was confirmed by two experiments. First, the catalyst (**1** and **5**) was filtered off the reaction mixture and the filtrate was heated for an additional 4 hours. No additional styrene oxide was converted consistent with the cessation of all catalytic activity. The filtrate was also examined by ICP-OES and less than 1 % of starting Al was observed. Second, recycling the catalysts was investigated. The aminolysis activity with reused xerogels

1 and **5** was unaffected in four consecutive 15 min. runs (26 ± 2%; 14 ± 2%, resp.). The performance of all catalysts in the aminolysis reaction is summarized in Table 3 (See also Table S1 for details).

All of the aluminosilicate xerogels prepared here exhibited catalytic activities comparable, and in most cases significantly superior to commercially available catalysts used for benchmarking (zeolite β and $SiO_2 \cdot Al_2O_3$ catalysts). The highest activities were observed for the materials containing 3-connected aluminum sites (**1**, **2** and **6**) (TOF = 248, 304 and 643 h^{-1}, respectively). The xerogel **1a** exhibited activity identical to that observed for xerogel **1** (TOF = 250 h^{-1}) consistent with our earlier conclusions based on spectroscopic data that they contained identical aluminum sites. Aluminosilicate **5**, containing 3C-Al←THF sites and the smaller cross-linking silane (Me_2SiCl_2) displayed much lower activity (TOF = 129 h^{-1}) than the corresponding catalysts (**2**, **6**) with the longer bridges. These data are consistent with our earlier observations of exchange reactions suggesting that xerogel **5** contains a significant number of inaccessible Al sites within its pore cavities.

Table 3 Catalytic Activities of Aluminosilicate Materials[a]

Sample	Conversion [%] (15 min)	Selectivity [%] Ia	IIa	TOF[b]
3C-Al←THF / −$SiMe_2$− (**5**)	9	90	10	129
3C-Al←THF / −CH_2CH_2− (**2**)	36	94	6	304
3C-Al←THF / −$CH_2CH_2CH_2$− (**6**)	27	93	7	643
3C-Al←Py / −CH_2CH_2− (**1**)	28	93	7	248
3C-Al←Py / −CH_2CH_2− (**1a**)	26	90	10	250
4C-Al·[NBu_4] / −CH_2CH_2− (**3**)	11	87	13	159
4C-Al· [HLut] / −CH_2CH_2− (**4**)	15	99	6	198
Blank – no catalyst	<1	-	-	-
Blank – Al-free silicate platform	<1	-	-	-
Blank – Al-free silicate platform	3 (60 min)	-	-	-
Zeolite β (H^+)	12	92	8	120
$SiO_2 \cdot Al_2O_3$ cat. support[c]	11	91	9	116
SiAlF1-500[26e]	50	97	3	100
SiAlP1-500[26e]	46	96	4	86

[a]Conditions: 5 mL toluene, 50°C, 25 mg catalyst; substrate: Al = 250, stir rate: 400 rpm; [b]TOF: apparent turnover frequency [h^{-1}] based on conversion of starting material at 15 minutes, assuming all aluminum sites in each catalyst are equivalent and functioning active sites; [c]Sigma-Aldrich grade 135

The turnover frequencies observed for xerogels **3** and **4** are lower than those observed for xerogels with 3-connected sites. We believe three factors must be considered in understanding these differences: the steric accessibility of the site, the charge on the aluminum center and the possible participation of the counterion. 4C-Al sites are expected to be significantly more sterically congested and less flexible in opening up coordination sites for substrates, presumably lowering both binding strength and rate or reaction. The charge on the aluminum center is also expected to be significantly different between 3C-Al (formally neutral) and 4C-Al (formally anionic) sites. This difference in charge would also affect each center's ability to function as a Lewis acid catalyst. Finally, in the case of 4C-sites, the counterions present may also contribute to their observed catalytic activities; $[nBuN]^+$ as a weak Lewis base and lutidinium as a weak Brønsted acid. Experiments to probe all of these factors are in progress.

Conclusions

In the work presented here we have demonstrated a targeted synthetic strategy for preparing specific types of aluminum sites active in catalysis within a silicate matrix. The central principles of this strategy are by no means limited to aluminum or the silicate cube described here. All that is needed are precursors to the desired active sites, a building block that will eventually become the surrounding matrix and a second set of linking groups that knit the final matrix together. In the case of the aluminosilicate catalysts described here, we have characterized the three- and four-connected aluminum centers via a broad range of spectroscopies and simple ligand exchange reactions, all of which lead to their description as porous, aluminosilicate matrices containing homogeneously dispersed, well defined active sites. By one measure of relative acidity (^{31}P NMR shift of TEPO), 3-connected "extraframework" aluminum sites in these xerogels are stronger Lewis acid sites than 4-connected "framework" aluminum sites. At the same time, ligand exchange studies show clear differences between "identical" sites which depend on the secondary linkers used to construct these matrices. Smaller, more rigid linkers (–$SiMe_2$–, xerogel **5**) appear to restrict access to the aluminum sites making some virtually inaccessible.

All of these xerogels function as catalysts in opening styrene oxide and exhibit activities that rival or are significantly higher than those previously reported for other aluminosilicate materials. 3-connected extraframework aluminum sites are more active than embedded 4-connected sites as Lewis acids in transforming styrene oxide into the corresponding amino alcohol. Finally, in parallel with ligand exchange behavior, the use of larger, more flexible secondary linkers in the synthesis of these matrices make all sites accessible leading to significantly higher catalytic activities. The accessibility of active sites has been an active topic of investigation in zeolite catalysis.[57, 58] In most case investigations have focussed on identifying different sites based on their chemical makeup as well as their accessibility. Here we describe how the accessibility of otherwise identical active sites can be rationally tuned at the time of synthesis.

This synthetic strategy for preparing single site catalysts opens the door to a number of interesting systems. Methods for transforming the 3- or 4-connected Lewis sites into Brønsted acids are easily imagined. Investigations into making boron and gallium analogues as well as replacing the counterions of the 4C-sites with other metal cations are in progress.

Acknowledgements

This material is based upon work supported by: 1) the Center for Direct Catalytic Conversion of Biomass to Biofuels (C3Bio), an Energy Frontier Research Center funded by the U.S. Department of Energy, Office of Science, Office of Basic Energy Sciences under Award Number DE-SC0000997; 2) the U.S. Department of Energy, Office of Science, Office of Basic Energy Sciences program (DE-FG02-01ER15259), and the DOE Nuclear Energy Research Program (DE-NE0008421).

References

[1] L. Wu, T. Moteki, A.A. Gokhale, D.W. Flaherty, F.D. Toste, Production of Fuels and Chemicals from Biomass: Condensation Reactions and Beyond, Chem, 1 (2016) 32-58.
[2] A.A. Latimer, A.R. Kulkarni, H. Aljama, J.H. Montoya, J.S. Yoo, C. Tsai, F. Abild-Pedersen, F. Studt, J.K. Norskov, Understanding trends in C-H bond activation in heterogeneous catalysis, Nat. Mater., 16 (2017) 225-229.
[3] J.M. Thomas, The concept, reality and utility of single-site heterogeneous catalysts (SSHCs), Phys. Chem. Chem. Phys., 16 (2014) 7647-7661.
[4] K. Reuter, C.P. Plaisance, H. Oberhofer, M. Andersen, Perspective: On the active site model in computational catalyst screening, J. Chem. Phys., 146 (2017) 040901-040908.
[5] R.A.v. Santen, Modeling Catalytic Reactivity in Heterogeneous Catalysis, in: R.A.V.S.a.P. Sautet (Ed.) Computational Methods in Catalysis and Materials Science, Wiley-VCH, Weinheim, Germany, 2009.

[6] M. Neurock, Theory and Simulation in Catalysis, in: R. Davis (Ed.) Catalysis by Nanostructured Materials, Imperial College Press, Hackensack, NJ, 2011, pp. 91-150.
[7] Modern Surface Organometallic Chemistry, J.-M. Basset, R. Psaro, D. Roberto, R. Ugo ed., Wiley-VCH, Darmstadt, 2009.
[8] C. Copéret, A. Comas-Vives, M.P. Conley, D.P. Estes, A. Fedorov, V. Mougel, H. Nagae, F. Núñez-Zarur, P.A. Zhizhko, Surface Organometallic and Coordination Chemistry toward Single-Site Heterogeneous Catalysts: Strategies, Methods, Structures, and Activities, Chem. Rev., 116 (2016) 323-421.
[9] P.K. Jal, S. Patel, B.K. Mishra, Chemical modification of silica surface by immobilization of functional groups for extractive concentration of metal ions, Talanta, 62 (2004) 1005–1028.
[10] C.E. Bronnimann, R.C. Zeigler, G.E. Macie, Proton NMR Study of Dehydration of the Silica Gel Surface, J. Am. Chem. Soc., 110 (1988) 2023-2026.
[11] V. Dal Santo, F. Liguori, C. Pirovano, M. Guidotti, Design and Use of Nanostructured Single-Site Heterogeneous Catalysts for the Selective Transformation of Fine Chemicals, Molecules, 15 (2010) 3829-3856.
[12] E.T.C. Vogt, B.M. Weckhuysen, Fluid catalytic cracking: recent developments on the grand old lady of zeolite catalysis, Chem. Soc. Rev., 44 (2015) 7342-7370.
[13] G. Busca, Acid catalysts in industrial hydrocarbon chemistry, Chem. Rev., 107 (2007) 5366-5410.
[14] V. Blay, B. Louis, R. Miravalles, T. Yokoi, K.A. Peccatiello, M. Clough, B. Yilmaz, Engineering Zeolites for Catalytic Cracking to Light Olefins, ACS Catalysis, 7 (2017) 6542-6566.
[15] Z. Wang, Y. Jiang, O. Lafon, J.a. Trbosc, Brønsted acid sites based on penta-coordinated aluminum species, Nat. Commun., 7 (2016) 13820.
[16] T. Yashima, K. Sato, T. Hayasaka, N. Hara, Alkylation on synthetic zeolites: III. Alkylation of toluene with methanol and formaldehyde on alkali cation exchanged zeolites, J. Catal., 26 (1972) 303-312.
[17] J.C. Kim, K. Cho, S. Lee, R. Ryoo, Mesopore wall-catalyzed Friedel-Crafts acylation of bulky aromatic compounds in MFI zeolite nanosponge, Catal. Today, 243 (2015) 103-108.
[18] M. Onaka, N. Hashimoto, Y. Kitabata, R. Yamasaki, Aluminum-rich mesoporous aluminosilicate (Al-HMS) as a solid acid catalyst for the Diels–Alder reaction of acrylates with 1,3-dienes, Appl. Catal., A, 241 (2003) 307-317.
[19] D.P. Debecker, C. Boissire, G. Laurent, S. Huet, P. Eliaers, C. Sanchez, R. Backov, B. Bujoli, Z. Gan, G. Hoatson, First acidic macro-mesocellular aluminosilicate monolithic foams “SiAl(HIPE)” and their catalytic properties, Chem. Commun., 51 (2015) 14018-14021.
[20] J.R. Di Iorio, R. Gounder, Controlling the Isolation and Pairing of Aluminum in Chabazite Zeolites Using Mixtures of Organic and Inorganic Structure-Directing Agents, Chem. Mater., 7 (2016) 2236-2247.
[21] Y. Jiang, J. Huang, W. Dai, M. Hunger, Solid-state nuclear magnetic resonance investigations of the nature, property, and activity of acid sites on solid catalysts, Solid State Nucl. Magn. Reson., 39 (2011) 116-141.
[22] R. Duchateau, R.J. Harmsen, H.C.L. Abbenhuis, R.A. van Santen, A. Meetsma, S.K.H. Thiele, M. Kranenburg, Modeling Acidic Sites in Zeolites and Aluminosilicates by Aluminosilsesquioxanes, Chem. Eur. J., 5 (1999) 3130-3135.
[23] M. Caillot, A. Chaumonnot, M. Digne, C. Poleunis, D.P. Debecker, J.A. van Bokhoven, Synthesis of amorphous aluminosilicates by grafting: Tuning the building and final structure of the deposit by selecting the appropriate synthesis conditions, Microporous Mesoporous Mater., 185 (2014) 179-189.
[24] A. Corma, Inorganic Solid Acids and Their Use in Acid-Catalyzed Hydrocarbon Reactions, Chem. Rev., 95 (1995) 559-614.
[25] W.E. Farneth, R.J. Gorte, Methods for Characterizing Zeolite Acidity, Chem. Rev., 95 (1995) 615-635.
[26] H.Y. Luo, J.D. Lewis, Y. Roman-Leshkov, Lewis Acid Zeolites for Biomass Conversion: Perspectives and Challenges on Reactivity, Synthesis, and Stability, Annu. Rev. Chem. Biomol. Eng., 7 (2016) 663-692.

[27] G.L. Woolery, H.C. Timken, J.C. Vartuli, On the nature of framework Brønsted and Lewis acid sites in ZSM-5, Zeolites, 19 (1997) 288-296.
[28] N.N. Ghosh, J.C. Clark, G.T. Eldridge, C.E. Barnes, Building block syntheses of site-isolated vandady groups in silicate oxides, Chem. Comm., (2004) 856-857.
[29] M.-Y. Lee, J. Jiao, R. Mayes, E. Hagaman, C.E. Barnes, The Targeted Synthesis of Single Site Vanadyl Species on the Surface and in the Framework of Silicate Building Block Materials, Catal. Today, 160 (2011) 153-164.
[30] J.C. Clark, C.E. Barnes, Reaction of the $Si_8O_{20}(SnMe_3)_8$ Building Block with Silyl Chlorides: A New Synthetic Methodology for Preparing Nanostructured Building Block Solids, Chem. Mater., 19 (2007) 3212-3218.
[31] M.Y. Lee, J. Jiao, R. Mayes, E. Hagaman, C.E. Barnes, The targeted synthesis of single site vanadyl species on the surface and in the framework of silicate building block materials, Catal. Today, 160 (2011) 153-164.
[32] F.J. Feher, K.J. Weller, Phosphorus(III)-containing silicates via a new aprotic building-block approach to multicomponent silicates, Chem. Mater., 6 (1994) 7-9.
[33] D.P. Debecker, V. Hulea, P.H. Mutin, Mesoporous mixed oxide catalysts via non-hydrolytic sol–gel: A review, Applied Catalysis A: General, 451 (2013) 192-206.
[34] Y. Song, Y. Huang, E.A. Havenga, I.S. Butler, Vibrational spectra of crystalline tetrakis(trimethylsilyl)silane(IV), $Si[Si(CH_3)_3]_4$, at high pressures, Vib. Spectrosc, 27 (2001) 127-134.
[35] M.J. Child, M.J. Heywood, G.H. Yong, C.H. Rochester, Brønsted Acidity of Silanol Groups on Silica Immersed in Carbon Tetrachloride, J. Chem. Soc., Faraday Trans., 78 (1982) 2005-2010.
[36] L. Oliviero, A. Vimont, J.-C. Lavalley, F. Romero-Sarria, M. Gaillard, F. Maug'e, 2,6-dimethylpyridine as a probe of the strength of Brønsted acid sites: study on zeolites. Application to alumina., Phys. Chem. Chem. Phys., 7 (2005) 1861-1869.
[37] C.S. Blackwell, Investigation of zeolite frameworks by vibrational properties. 1. The double-four-ring in group 3 zeolites, J. Phys. Chem., 83 (1979) 3251-3257.
[38] E.R.d. Sola, F. Estevan, F.J. Torres, J. Alarcón, Effect of thermal treatment on the structural evolution of 3:2 and 2:1 mullite monophasic gels, J. Non-Cryst. Solids, 351 (2005) 1202-1209.
[39] Y. Hirata, K. Sakeda, Y. Matsushita, K. Shimada, Y. Ishihara, Characterization and Sintering Behavior of Alkoxide-Derived Aluminosilicate Powders, J. Am. Ceram. Soc., 72 (1989) 995-1002.
[40] I.S. Pieta, M. Ishaq, R.P.K. Wells, J.a. Anderson, Quantitative determination of acid sites on silica-alumina, Appl. Cat. A, 390 (2010) 127-134.
[41] M. Lefrancois, G. Malbois, The nature of the acidic sites on mordenite: Characterization of adsorbed pyridine and water by infrared study, J. Catal., 20 (1971) 350-358.
[42] C.H. And, A.C. Pierre, Influence of the Sol−Gel Acidic Synthesis Conditions on the Porous Texture and Acidity of SiO_2−Al_2O_3 catalysts with a Low Al Proportion, Langmuir, 16 (2000) 530-536.
[43] E. Masika, R. Mokaya, Mesoporous Aluminosilicates from a Zeolite BEA Recipe, Chem. Mater., 23 (2011) 2491-2498.
[44] M. Toba, F. Mizukami, S.-i. Niwa, T. Sano, K. Maeda, H. Shoji, Effect of preparation methods on properties of amorphous alumina/silicas, J. Mater. Chem., 4 (1994) 1131-1135.
[45] M.S. Bains, D.C. Bradley, Coordination Complexes of Metal Alkoxides Part I. Metal Alkoxide - Hydrazine Complexes, Can. J. Chem., 40 (1962) 1350-1354.
[46] A. Zheng, S.-J. Huang, S.-B. Liu, F. Deng, Acid properties of solids acid catalysts characterized by solid-state ^{31}P of adsorbed phosphorous probe molecules, Phys. Chem. Chem. Phys., 13 (2011) 14889-14901.
[47] J.P. Osegovic, R.S. Drago, Measurement of the Global Acidity of Solid Acids by ^{31}P NMR of Chemicsorbed Triethylphosphine Oxide, J. Phys. Chem. B, 104 (2000) 147-154.

[48] D. Margolese, J.A. Melero, S.C. Christiansen, B.F. Chmelka, D.D. Stucky, Direct Syntheses of Ordered SBA-15 Mesoporous Silica containing Sulfonic Acid Groups, Chem. Mat., 12 (2000) 2448-2459.
[49] C.E. Barnes, K. Sharp, A.A. Albert, M.E. Peretich, P. Fulvio, P.N. Ciesielski, B.S. Donohoe, Metal-silicate catalysts: Single site, mesoporous systems without templates, J. Nanosci. Lett., 5 (2015) 1-7.
[50] J.J. Morrison, C.J. Love, B.W. Manson, I.J. Shannon, R.E. Morris, Synthesis of functionalised porous network silsesquioxane polymers, J. Mater. Chem., 12 (2002) 3208-3212.
[51] Y. Hagiwara, A. Shimojima, K. Kuroda, Formation of Reactive Microporous Networks from Alkoxyvinylsilylated Siloxane Cages, Bull. Chem. Soc. Jpn., 83 (2010) 424-430.
[52] R. Kore, R. Srivastava, B. Satpati, Highly Efficient Nanocrystalline Zirconosilicate Catalysts for the Aminolysis, Alcoholysis, and Hydroamination Reactions, ACS Catalysis, 3 (2013) 2891-2904.
[53] M.W.C. Robinson, A.M. Davies, I. Mabbett, T.E. Davies, D.C. Apperley, S.H. Taylor, A.E. Graham, Synthesis of nanoporous aluminosilicate materials and their application as highly selective heterogeneous catalysts for the synthesis of β-amino alcohols, J. Mol. Catal. A: Chem., 329 (2010) 57-63.
[54] M.W.C. Robinson, D.A. Timms, S.M. Williams, A.E. Graham, A mild and efficient synthesis of β-amino alcohols from epoxides using a mesoporous aluminosilicate catalyst, 48 (2007) 6249-6251.
[55] R. Chakravarti, H. Oveisi, P. Kalita, R.R. Pal, S.B. Halligudi, M.L. Kantam, A. Vinu, Three-dimensional mesoporous cage type aluminosilicate: An efficient catalyst for ring opening of epoxides with aromatic and aliphatic amines, Microporous Mesoporous Mater., 123 (2009) 338-344.
[56] D. Skoda, A. Styskalik, Z. Moravec, P. Bezdicka, M. Babiak, M. Klementova, C.E. Barnes, J. Pinkas, Novel non-hydrolytic templated sol-gel synthesis of mesoporous aluminosilicates and their use as aminolysis catalysts, RSC Advances, 6 (2016) 24273-24284.
[57] J. Dijkmans, M. Dusselier, W. Janssens, M. Trekels, A. Vantomme, E. Breynaert, C. Kirschhock, B.F. Sels, An Inner-/Outer-Sphere Stabilized Sn Active Site in β-Zeolite: Spectroscopic Evidence and Kinetic Consequences, ACS Catalysis, 6 (2016) 31-46.
[58] V.L. Sushkevich, D. Palagin, I.I. Ivanova, With Open Arms: Open Sites of ZrBEA Zeolite Facilitate Selective Synthesis of Butadiene from Ethanol, ACS Catalysis, 5 (2015) 4833-4836.